Classification of Parkinson's disease with dementia using phase locking factor of event-related oscillations to visual and auditory stimuli

Journal of Neural Engineering

PAPER

Classification of Parkinson's disease with dementia using phase locking factor of event-related oscillations to visual and auditory stimuli

Emine Elif Tülay[1,*], **Ebru Yıldırım**[2,3], **Tuba Aktürk**[2,3,4] and **Bahar Güntekin**[2,5]

[1] Department of Software Engineering, Faculty of Engineering, Muğla Sıtkı Koçman University, Muğla, Turkey
[2] Research Institute for Health Sciences and Technologies (SABITA), Regenerative and Restorative Medicine Research Center (REMER), Clinical Electrophysiology, Neuroimaging and Neuromodulation Lab, Istanbul Medipol University, Istanbul, Turkey
[3] Vocational School, Program of Electroneurophysiology, Istanbul Medipol University, Istanbul, Turkey
[4] Department of Cognitive Neuroscience, Faculty of Psychology and Neuroscience, Maastricht University, Maastricht, The Netherlands
[5] Department of Biophysics, School of Medicine, Istanbul Medipol University, Istanbul, Turkey
* Author to whom any correspondence should be addressed.

E-mail: eliftulay@mu.edu.tr

Keywords: Parkinson's disease with dementia, delta, theta, inter-trial phase coherence, classification, linear discriminant analysis

OPEN ACCESS

RECEIVED
8 October 2022

REVISED
24 January 2023

ACCEPTED FOR PUBLICATION
21 March 2023

PUBLISHED
31 March 2023

Abstract

Objective. In the last decades, machine learning approaches have been widely used to distinguish Parkinson's disease (PD) and many other neuropsychiatric diseases. They also speed up the clinicians and facilitate decision-making for several conditions with similar clinical symptoms. The current study attempts to detect PD with dementia (PDD) by event-related oscillations (EROs) during cognitive processing in two modalities, i.e. auditory and visual. *Approach.* The study was conducted to discriminate PDD from healthy controls (HC) using event-related phase-locking factors in slow frequency ranges (delta and theta) during visual and auditory cognitive tasks. Seventeen PDD and nineteen HC were included in the study, and linear discriminant analysis was used as a classifier. During classification analysis, multiple settings were implemented by using different sets of channels (overall, fronto-central and temporo-parieto-occipital (TPO) region), frequency bands (delta-theta combined, delta, theta, and low theta), and time of interests (0.1–0.7 s, 0.1–0.5 s and 0.1–0.3 s for delta, delta-theta combined; 0.1–0.4 s for theta and low theta) for spatial-spectral-temporal searchlight procedure. *Main results.* The classification performance results of the current study revealed that if visual stimuli are applied to PDD, the delta and theta phase-locking factor over fronto-central region have a remarkable contribution to detecting the disease, whereas if auditory stimuli are applied, the phase-locking factor in low theta over TPO and in a wider range of frequency (1–7 Hz) over the fronto-central region classify HC and PDD with better performances. *Significance.* These findings show that the delta and theta phase-locking factor of EROs during visual and auditory stimuli has valuable contributions to detecting PDD.

1. Introduction

Among neurodegenerative disorders, Parkinson's disease (PD) ranks after Alzheimer's disease (AD) as the second most common disorder, with nearly ten million people worldwide (Khoshnevis and Sankar 2021), and due to the aging population, the estimated prevalence of PD will increase in the coming years. Although PD is mostly known as a motor disorder, it is a multi-system disease including both motor and non-motor symptoms (Aarsland *et al* 2017, Güntekin *et al* 2020). The cognitive decline that affects different domains, including attention, working memory, and visuospatial skills, is the most common non-motor symptoms symptom of PD, and it has a severe and negatively influences on the quality of life (Hinnell and Chaudhuri 2009, Tolosa *et al* 2021). According to long-term follow-up studies in literature, approximately half of PD patients evolve into PD dementia (PDD) in ten years (Williams-Gray *et al* 2013), but the ratio increases to 83% with the longer duration of the disease if they survive (Hely *et al* 2008). Therefore,

early and accurate diagnosis becomes a crucial issue to mitigate its complications.

Non-motor symptoms like cognitive changes mostly have been used as supportive diagnostic criteria. However, there are recently published studies that revealed the contribution of sleep features (Bestwick *et al* 2021, Yang *et al* 2022), olfactory functions (Tremblay *et al* 2020, Bestwick *et al* 2021), and social functioning (Yu *et al* 2022) to detect PD although Mei *et al* (2021) mentioned that non-motor symptoms are not yet valid for independently diagnosing PD. On the other hand, motor symptoms are a late manifestation of early diagnosis (Maitín *et al* 2020). Clinical evaluation and neuropsychological assessment batteries are used to detect cognitive impairment in PD. Nevertheless, neuropsychological assessment batteries may not be sensitive enough, especially at the early stages. Besides, inevitably, it can appear as an evaluation tool open to the subjective interpretation of the practitioner. Various studies use neuroimaging techniques like functional magnetic resonance imaging (fMRI), Positron-Emission Tomography/Single-photon emission computed tomography (PET/SPECT), magnetoencephalogram (MEG), and electroencephalogram (EEG) to investigate cognitive impairment in PD (Weingarten *et al* 2015, Shirahige *et al* 2020). However, the interpretation of findings and identification of biomarkers is not an easy process, therefore, it needs the expertise to distinguish the disease precisely and objectively (Alzubaidi *et al* 2021). Moreover, different neurophysiological features should be evaluated to obtain straightforward and robust results. Considering all these reasons, there is a need for an objective tool that will increase sensitivity in diagnosis and clinical evaluation, and neuropsychological tests performed by the specialist.

Especially in the last decade, machine learning (ML) techniques have made quite a splash because of the improvements in computing technology and are started to be widely used as computer-aided diagnosis tools for distinguishing many neuropsychiatric diseases (Raghavendra *et al* 2019, Tulay *et al* 2019, Chen *et al* 2022), also they can speed up the clinicians and facilitate decision-making for several conditions with similar clinical symptoms. There are various studies that use different neuroimaging techniques, ML models, and feature extraction methods for detecting PD (please see the reviews, Bind *et al* 2015, Pereira *et al* 2019, Khachnaoui *et al* 2020, Mei *et al* 2021, Radha *et al* 2021, Saravanan *et al* 2022).

EEG is the most used neuroimaging technique for classification studies in PD due to its being technically and economically more practical (Maitín *et al* 2020). A large majority of the studies have been focused on resting-state data (Chaturvedi *et al* 2017, Yuvaraj *et al* 2018, Anjum *et al* 2020, Oh *et al* 2020, Aljalal *et al* 2022, Chang *et al* 2022, Yang and Huang 2022), event-related potentials (Wang *et al* 2020, Hassin-Baer *et al* 2022) and other time domain characteristics of EEG (Coelho *et al* 2023) as features of classifiers for the diagnosis of PD based on EEG. However, there is vast literature supporting the association between event-related oscillations (EROs) in specific frequency ranges and specific cognitive domains (Başar-Eroğlu *et al* 1992, Başar *et al* 1999, 2001, Klimesch 1999, Demiralp *et al* 2000, 2001, Başar-Eroğlu and Demiralp 2001).

Across years of research, event-related delta and theta oscillations elicited by an oddball task have been linked with several cognitive functions like perception, attention, decision-making, and working memory (please see the reviews; Harmony 2013, Güntekin and Başar 2016, Karakaş *et al* 2020). EROs also provide a promising methodology to observe abnormalities of cognitive processes in PD and PDD as well as other dementia types such as AD (Güntekin *et al* 2022). Studies revealed that cognitively normal PD patients had reduced delta responses than healthy controls (HC) upon application of visual (Emek Savaş *et al* 2017) and auditory (Güntekin *et al* 2018) target stimulation. In addition, delta ERO during auditory target stimuli decreases in PDD as well (Güntekin *et al* 2018). Event-related spectral perturbation (ERSP) (Delorme and Makeig 2004) and inter-trial phase coherence (ITPC, also referred to as inter-trial coherence) (van Diepen and Mazaheri 2018) are other two important measurements of oscillatory activities to understand mechanisms of cognitive processes. According to the results of the studies in the literature, ERSP and ITPC in delta and theta frequency bands can be distinctive for PD patients with mild cognitive impairment (MCI) (Yener *et al* 2019) and PDD (Güntekin *et al* 2020).

A few studies use EROs in response to cognitive tasks to detect PD by using an ML approach (Cavanagh *et al* 2018, Singh *et al* 2018, Vanegas *et al* 2018). To the best of our knowledge, there is a big gap in identifying PDD patients via ML approaches upon application of a cognitive task. The current study aimed to examine mainly two aspects of the classification of PDD. First, to attempt to close the gap via ITPC measurements obtained upon application of visual and auditory cognitive tasks as features of the classification model. Second, to detect the best spatial-spectral-temporal feature set among different modalities of cognitive tasks, frequency bands, time ranges, and brain areas to classify PDD. In this way, we could provide the electrophysiological clue that would form the basis of the hypothesis that could be focused on in future studies investigating the classification of subtypes of PD patients with different levels of cognitive impairment. For this purpose, linear discriminant analysis (LDA) was used. We hypothesized that PDD patients would be discriminated with the delta and theta ITPC values in response to target stimulation of visual cognitive task in especially frontocentral regions.

2. Method and materials

2.1. Participants

A total of 36 participants were included in the study and there were two groups, PDD and healthy elderly controls. Seventeen PDD patients and nineteen healthy elderly controls who had no cognitive impairment were included in the study. PDD patients were diagnosed according to clinical examination using UK Parkinson's Disease Society Brain Bank Diagnostic Criteria for PD (Daniel and Lees 1993), and for the diagnosis of dementia in PD, Emre *et al* (2007)'s criteria were followed. The local ethical committee approved the present study (Istanbul Medipol University, Ethical report no: 10840098-51). Also, all participants and/or their relatives signed the informed consent form.

A detailed neuropsychological assessment test battery was applied to all participants in both PDD and HC groups. Within the scope of the neuropsychological test battery, the Turkish version of the standardized Mini-Mental State Examination (MMSE) (Folstein *et al* 1975, Güngen *et al* 2002), the Öktem Verbal Memory Processes test (Tanör 2011), the verbal fluency tests (Parker and Crawford 2018), Clinical Dementia Rating scale (CDR) (Morris 1993, 1997) were employed to assess the general cognitive states of the participants, memory functions, executive functions, and staging of dementia, respectively. Additionally, the Geriatric Depression Scale (GDS) (Yesavage *et al* 1982) was used to check for any signs of depression. Moreover, the Neuropsychiatric Inventory (NPI) evaluating the impact of neuropsychiatric symptoms and the REM Sleep Behavior Disorder Screening Questionnaire (RBD) assessing REM Sleep Behavior Disorder (Stiasny-Kolster *et al* 2007) were applied to PDD group. Furthermore, the unified Parkinson's disease rating scale (UPDRS) (Movement Disorder Society Task Force on Rating Scales for Parkinson's Disease 2003) and Hoehn and Yahr scale (Hoehn and Yahr 1967) were applied to PDD patients to assess motor symptoms associated with PD. A neurologist evaluated all participants at Istanbul Medipol University Hospital in terms of diagnosis, exclusion, and inclusion criteria.

Table 1 shows the demographic and clinical characteristics of the groups. As seen in table 1, the mean ages were 71.23 (SD: 6.81) and 66.89 (SD: 6.35) years for PDD and HC groups, respectively ($p = .061$). In our study, there were 17 men in the PDD group, whereas 12 men and 7 women were in the HC group. The mean education years were 5.47 (SD: 5.33) and 8.37 (SD: 5.00) years for PDD and HC groups, respectively ($p = .146$). Moreover, the mean MMSE scores were 19.18 (SD: 3.56) and 27.21 (SD: 1.62) for PDD and HC groups, respectively ($p < .0001$). The mean GDS score were 10.35 (SD: 6.22) and 6.10 (SD: 6.93) for PDD and HC groups, respectively ($p = .028$). The mean scores of UPDRS (only motor score), NPI, and RBD were 27.87 (SD: 9.62), 23.47 (SD: 17.01), and 4.47 (SD: 3.45) for the PDD patients, respectively. The Mann–Whitney U test was used for group comparisons of demographics (table 1).

Fifteen patients of the PDD group were mild dementia and two patients were moderate dementia according to the CDR scale. In the PDD group, a patient was in stage 1 and six patients were in stage 2 according to Hoehn and Yahr scale. Moreover, two patients were in stage 2.5 and five patients were in stage 3. Furthermore, two patients were in stage 4 (table 1).

The inclusion criteria for the PDD group were MMSE scores lower than 26, CDR scores higher than 0.5, and impaired daily living activities. Furthermore, another inclusion criterion was having a cognitive impairment as defined with performance $\geqslant$1.5 standard deviations shift from the norm values in the neuropsychological assessment tests. The exclusion criteria for PDD patients were the presence of dementia such as vascular dementia, Frontotemporal dementia, dementia with Lewy body, or other types of dementia, alcohol and/or drug abuse, history of stroke and traumatic brain injury, presence of epilepsy, history of psychiatric disease, history of any other neurological disease except for PD, seconder parkinsonism such as cerebrovascular parkinsonism and drug-induced parkinsonism, atypical parkinsonism with absent or minimal responses to antiparkinsonian drugs. It permitted the use of PD-related medications for PDD patients. All PDD patients were evaluated after taking their daily LevoDopa (equivalent) dose.

The inclusion criteria for the HC group were as follows; MMSE score $\geqslant$26, no diagnosed neurological and/or psychiatric disease, and no use of neurological and/or psychiatric drugs. The exclusion criteria for the HC group were the presence of dementia (frontotemporal dementia, vascular dementia, dementia with Lewy body, PDD, AD dementia, etc), history of head trauma, psychiatric and/or neurological disease, presence of epilepsy, and use of medications affecting cognitive performance, alcohol and/or drug abuse.

2.2. Experimental task

In the current study, the auditory and visual oddball paradigms were applied to participants during EEG recording. In the auditory oddball paradigm, there were two types of sound with different frequencies named target (1600 Hz) and nontarget stimuli (1500 Hz). In total, there were 120 stimuli which included 40 target stimuli and 80 nontarget stimuli (figure 1). The sound intensity was 80 dB for both stimulus types. In the visual oddball paradigm, there were again two types of stimuli (target and nontarget) with different luminance, and the luminance of target was 40 cd m^{-2}, whereas the luminance of nontarget was 10 cd m^{-2}. In total, there were 120 stimuli which

Table 1. The clinical and demographic and clinical characteristics of the participants.

	HC Mean ± SD	PDD Mean ± SD	*p*
Age (year)	66.89 ± 6.35	71.23 ± 6.81	.061
Education (year)	8.37 ± 5.00	5.47 ± 5.33	.146
MMSE	27.21 ± 1.62	19.18 ± 3.56	<.0001
GDS	6.10 ± 6.93	10.35 ± 6.22	.028
UPDRS (motor score)	—	27.87 ± 9.62	—
NPI	—	23.47 ± 17.01	—
RBD	—	4.47 ± 3.45	—
	HC (n)	PDD (n)	
CDR (mild/moderate/severe dementia)	—	15/2/0	—
Hoehn and Yahr stage (stage 1/2/2.5/3/4)	—	1/6/2/5/2	—

MMSE: Mini–Mental State Examination; UPDRS: Unified Parkinson's Disease Rating Scale; CDR: Clinical Dementia Rating scale; NPI: Neuropsychiatric Inventory; RBD: REM Sleep Behavior Disorder; Mann–Whitney *U* test; SD: standard deviation; n: noun; $p < .05$.

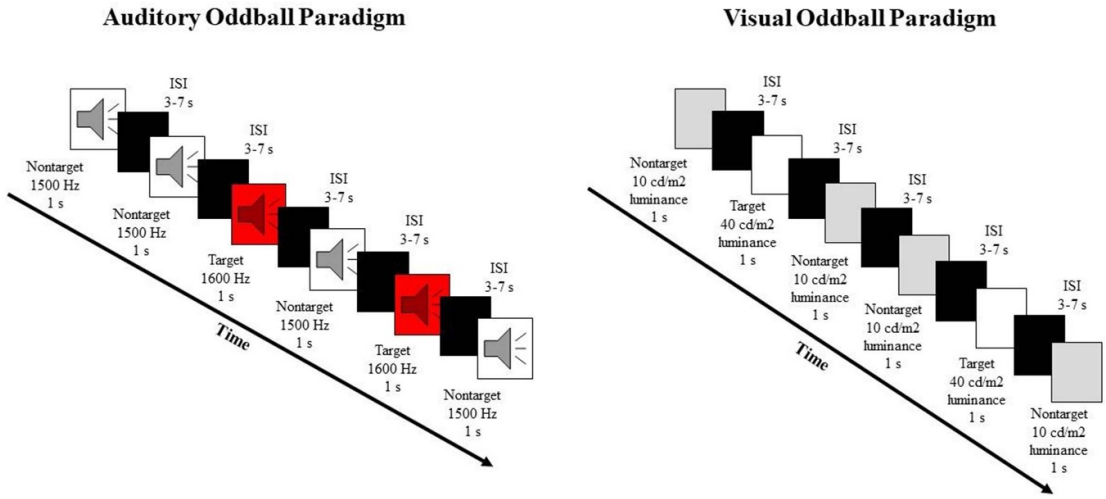

Figure 1. Experimental designs for auditory and visual oddball paradigms.

included 40 target stimuli and 80 nontarget stimuli (figure 1).

The stimuli were presented at full size on a 19 inch computer monitor with a refresh rate of 60 Hz. All stimuli were presented to participants randomly and with 1 s duration. The inter-stimulus interval varied between 3 and 7 s. The subjects mentally counted the target stimuli in both paradigms. The number of stimuli counted by the subjects was noted at the end of the paradigms.

2.3. EEG recording

EEGs of participants were recorded in an isolated Faraday room dimly lit by using Brain Amp 32-Channel DC System (Brain Products, Munich, Germany). During EEG recording, the sampling rate was 500 Hz, and band limits were 0.01 and 250 Hz. The elastic cap (Easy Cap) where 32 Ag–AgCl electrodes were mounted according to the international 10–20 system was used for EEG recordings. Additionally, the two linked electrodes (A1 + A2) were placed on the earlobes and served as references for all electrodes. In addition, the participants were requested to look at the screen without moving their eyes too much during the recording to minimize eye movements as well as the electro-oculogram (EOG) that was placed in the medial upper, and lateral orbital rim of the right eye was registered to detect eye movements. The impedance values of electrodes were kept below 10 kΩ (kiloohm).

2.4. EEG data analysis

Preprocessing and feature extraction steps of EEG data analysis were fulfilled using two different software. Preprocessing was performed via BrainVision Analyzer (Brain Products GmbH, Munich, Germany) and feature extraction was performed via FieldTrip Toolbox (version no: 20220104) (Oostenveld *et al* 2011) running under Matlab R2018b (MathWorks, Natick, MA, U.S.A).

2.4.1. Preprocessing

EEG data were analyzed for visual and auditory oddball, separately. Firstly, the continuous raw data were filtered (infinite impulse response filters: 0.01–60 Hz), and then the filtered continuous data were decomposed into distinct components using independent component analysis (ICA) to detect and remove artifacts caused by eye movements. The restricted infomax algorithm was used in the calculation of ICA. All recorded EEG and EOG channels (32 channels) were chosen for the ICA decomposition. The number of computed ICA components was equal to the number of chosen channels. ICA was conducted in semi-automatic mode. Each component was carefully checked, and regarding their topology, voltage ranges, and the improvement in the data that resulted from the extraction of these components, components for the horizontal and vertical eye movements were removed. After the removal of the detected components (these components were set to zero), the remaining components were composed with the inverse ICA analysis. The maximum component number removed for a subject was two. Afterward, continuous data were divided into epochs according to the stimulus onset (3000 ms before and 3000 ms after the stimulus) to avoid boundary effects in time-frequency analysis (Herrmann *et al* 2005). Manual artifact rejection was employed for the segmented data to clean the remaining artifacts. In this step, all data were manually checked, epoch by epoch. Accordingly, epochs with artifacts (e.g. remaining eye movement-related artifacts) were excluded. The remained epoch numbers were equalized for target and nontarget stimuli. Finally, the preprocessed data were exported for further analysis.

2.4.2. Feature extraction: ITPC analysis

ITPC which was first introduced as 'phase-locking factor' by Tallon-Baudry *et al* (1996) is a measure of the appearance and degree of consistency over trials within the range of zero to one. If the ITPC value is close to zero, it means that there is a high variability of phase angles across trials, whereas an ITPC value of 1 reflects all trials having the same phase angle (Delorme and Makeig 2004). As Makeig *et al* (2004) mentioned, ITPC is a useful measurement to model event-related brain dynamics. In the current study, ITCP values were extracted from the EEG data and used as features for the classifiers.

Before the extraction process, segmented data exported from the BrainVision Analyzer software were imported to the Matlab Platform by using custom-written scripts via the FieldTrip toolbox. After that, ITPC[6] values were computed for both visual and auditory target trials over each EEG channel and for all participants after the sensor-level time-frequency decomposition with complex Morlet wavelets was conducted on each trial of preprocessed data. A Morlet function with three cycles was used to calculate the time-frequency transform between 1 and 15 Hz with 0.5 Hz frequency resolution and the wavelet coefficients were estimated for 10 ms steps between −3 s and 3 s. Then, these ITPC values were used as the feature vector of the classifier.

2.5. Classification analysis

A Matlab toolbox for multivariate pattern analysis (MVPA), fieldtrip integrated MVPA-light toolbox (Treder 2020), was used to assess whether the EEG features could be decoded to predict the two groups, PDD and HC. LDA classifier with default hyperparameters[7] of MVPA-light toolbox was employed to differentiate PDD and HC via ITPC of EROs in response to visual and auditory target stimulation, separately.

To avoid the flow of information from the test set flowing into the processing of the train set, nested *z*-scoring was used as a preprocessing step prior to training the classifier. LDA was trained in ten-fold cross-validation and applied for each time-frequency point separately and for the average of time-frequency points in a specific time and frequency ranges using channels as features. The entire cross-validation was repeated five times with new randomly assigned folds to reduce the bias and ensure the robustness of the trained model. Then, the final result was calculated by averaging across all test folds and repetitions. The performance of the classifier was evaluated using multiple metrics, including confusion matrix, accuracy, Area under the ROC Curve (AUC), precision, recall, and F1 score (figure 2).

During classification analysis, multiple settings were implemented by using different sets of channels, frequency bands, and time of interest for the spatial-spectral-temporal searchlight procedure (figure 2) which is a technique to investigate which features contribute most to classification performance by performing a separate classification for each element of the searchlight dimension. These dimensions could be time and frequency as well as the channel (location) (Treder 2020). In the initial stage, all channels were included as features in the 1–7 Hz frequency band which involves both delta and theta bands and delta (1–4 Hz) frequency band with different time windows of interest (0.1–0.7 s, 0.1–0.5 s, and 0.1–0.3 s), also at theta (4–8 Hz) and low theta (4–6 Hz) frequency bands with 0.1–0.4 s time window of interest. The time windows and frequency ranges were determined by visual inspection of grand averages as well as accuracy tables obtained for each frequency–time point in 1 −10 Hz and at 0.1–0.9 s time window (please see figure 3). Then, in the light of

[6] www.fieldtriptoolbox.org/faq/itc/

[7] https://github.com/fieldtrip/fieldtrip/blob/master/ft_statistics_mvpa.m

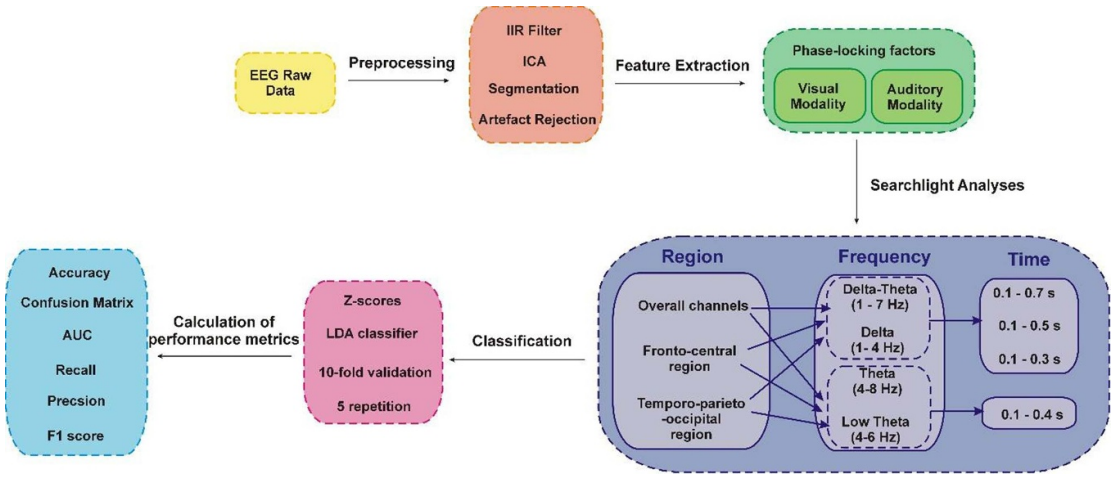

Figure 2. The pipeline of the classification analysis.

the literature on EROs during a cognitive task (please see section 1), all the processes were repeated for the special region of interest (ROI) which was the fronto-central area (F7, F3, Fz, F4, F8, FC3, FCz, FC4, C3, Cz, C4). Also, according to the visual inspection of classification accuracies for each channel in topographic plots (please see figure 5), the special ROI which was the temporo-parieto-occipital (TPO) area (T7, C3, Cz, C4, T8, TP7, CP3, CPz, CP4, TP8, P7, P3, Pz, P4, P8, O1, Oz, O2) were used as features for the separate run.

This searchlight procedure for the classification approach has been applied to the data collected and analyzed in previous studies by Güntekin *et al* (2018) and Güntekin *et al* (2020).

3. Results

After calculating complex Fourier-spectra in the 1–15 Hz frequency range by means of the wavelet transform, ITPC values for the targets of the visual and auditory oddball paradigms were calculated for each participant (see section 2.4.2). The grand averages are presented in the left box of figure 3, which includes topographic distributions in the 1–7 Hz frequency range and at the 0.1–0.7 s time window over all electrodes. According to the topographic plots, especially the fronto-central region seems a distinguishing feature of PDD in both paradigms. The middle box of figure 3 depicts the grand averages of ITPC values over the averaged across all electrodes in the visual and auditory modality for both HC and PDD. The plots give us clues for the frequency and time ranges in order to perform spectral-temporal searchlight analyses for the classification process (please see section 2.5). The classification results are presented by means of accuracy performance metrics for each time-frequency point separately using all channels as features (figure 3—right box) and help to identify which time-frequency point discriminative information shows up. The upper accuracy table in figure 3—right box shows that in the classification of HC and PDD, the higher performances were reached in the frequencies up to 7 Hz and at a latency between 0 and 0.7 s for visual modality. However, bottom accuracy table in figure 3—right box, which is for auditory modality, the higher performances are more localized and obtained in the 0.2–0.6 s time window for delta frequency band up to 2 Hz and in the quite early time window for the theta (4–8 Hz) frequency band.

Figure 4 depicts the results of the classification analyses by means of the accuracy metric by specifying different time–frequency points, where all channels were used as features. Figure 4(A) represents the accuracy values for visual and auditory delta (1–4 Hz) and delta-theta combined (1–7 Hz) as the frequency of interest at three different times of interest (0.1–0.3 s, 0.1–0.5 s, and 0.1–0.7 s). Figure 4(B) represents the accuracy values for visual and auditory theta (4–8 Hz) and low theta (4–6 Hz) as the frequency of interest at 0.1–0.4 s time window. As seen from the bar graph (figure 4(A)), the application of visual stimulation distinguish PDD with higher accuracies than auditory stimulation for all time and frequency of interest. Also, while the 0.1–0.3 s time window gives better accuracy values than the other time windows upon the application of visual target stimuli, auditory target stimulation causes higher values in a wider range of time window (0.1–0.7 s). To identify PDD, the classification performance for low theta is better than theta for both paradigms (figure 4(B)). Moreover, in the case that all the channels were used as features, the delta frequency band has more distinctive than the other frequency bands to predict PDD.

The classification steps were also re-run for the fronto-central and TPO regions for the same frequency and time windows to find the best predictive feature vector. All the classification metrics

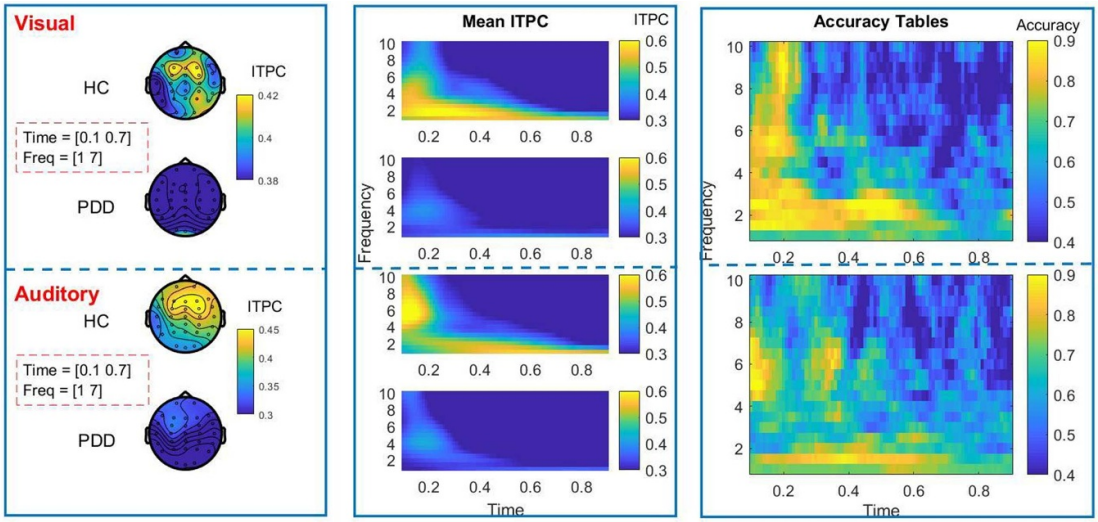

Figure 3. Results upon application of the target stimuli during visual oddball paradigm (upper row) and auditory oddball paradigm (bottom row). Left box: topographic maps of averaged ITPC values in 1–7 Hz and at 0.1–0.7 s over all electrodes for HC and PDD. Middle box: time-frequency representations: grand average of ITPC values in low frequency bands, delta and theta, over the averaged across all electrodes. Right box: plots yield (frequency × time) matrix of classification accuracies using all channels as features (HC vs PDD). HC: healthy controls, PDD: Parkinson's disease with dementia.

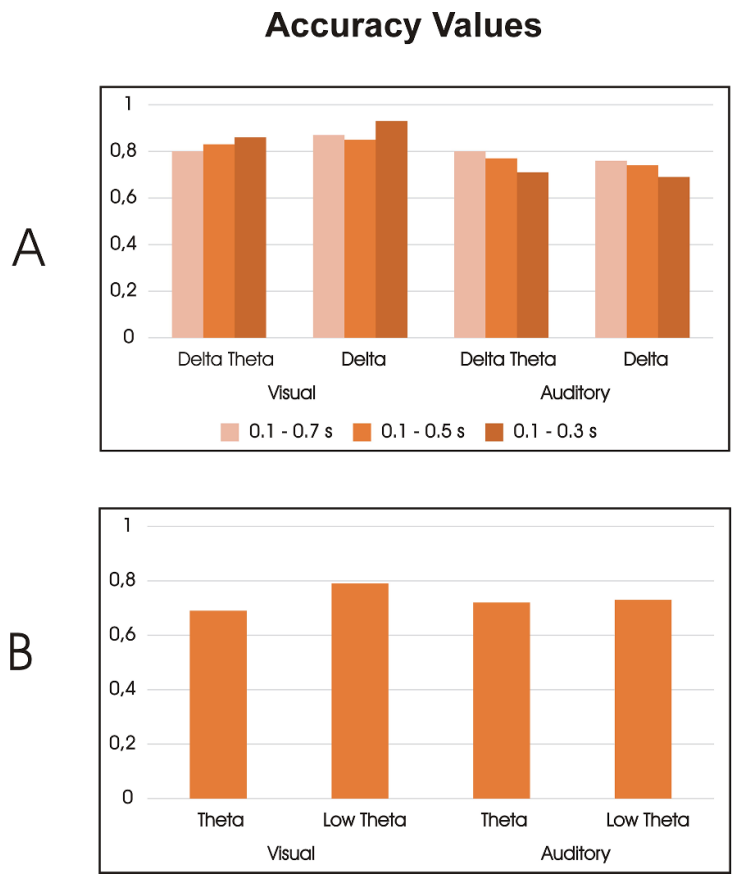

Figure 4. The classification accuracies for different times and frequencies where all channels were used as features.

(accuracy, AUC, confusion matrix, f1 score, precision, and recall) obtained by running spatial-spectral-temporal searchlight analyses are summarized in table 2 for event-related visual target ITPC and table 3 for event-related auditory target ITPC.

Table 2 shows that when all channels are used as features, the highest accuracies achieved for visual delta (0.93) and delta-theta combined (0.86) are in the 0.1–0.3 s time window whereas for auditory delta (0.76) and delta-theta combined (0.80) are in the 0.1–0.7 s time window (table 3). Also, theta shows a lower

Table 2. Classification metrics for visual target stimulation after running spatial-spectral-temporal searchlight analyses.

	Visual target								
ROI	Frequency band	Time windows	Acc	Acc_std	TP/TN	AUC	f1 score	Precision	Recall
All channels	Delta theta	0.1–0.7 s	0.80	0.18	0.88/0.72	0.97	0.82	0.86	0.85
		0.1–0.5 s	0.83	0.21	0.87/0.76	0.92	0.85	0.85	0.89
		0.1–0.3 s	0.86	0.16	0.87/0.88	0.92	0.84	0.90	0.84
	Delta	0.1–0.7 s	0.87	0.17	0.84/0.92	0.96	0.83	0.87	0.84
		0.1–0.5 s	0.85	0.19	0.84/0.82	0.94	0.84	0.89	0.84
		0.1–0.3 s	0.93	0.15	0.95/0.93	0.98	0.94	0.94	0.95
	Theta	0.1–0.4 s	0.69	0.22	0.76/0.70	0.86	0.64	0.64	0.71
	Low theta	0.1–0.4 s	0.79	0.21	0.80/0.75	0.87	0.80	0.82	0.84
Fronto-central channels	Delta theta	0.1–0.7 s	0.85	0.20	0.86/0.83	0.96	0.85	0.87	0.88
		0.1–0.5 s	0.91	0.13	0.90/0.94	0.97	0.90	0.96	0.88
		0.1–0.3 s	0.92	0.13	0.89/0.93	0.97	0.90	0.94	0.89
	Delta	0.1–0.7 s	0.88	0.19	0.89/0.88	0.93	0.88	0.91	0.90
		0.1–0.5 s	0.88	0.16	0.88/0.93	0.94	0.86	0.93	0.84
		0.1–0.3 s	0.94	0.11	0.95/0.94	0.95	0.95	0.96	0.95
	Theta	0.1–0.4 s	0.82	0.20	0.77/0.88	0.88	0.80	0.87	0.79
	Low theta	0.1–0.4 s	0.87	0.14	0.87/0.91	0.97	0.85	0.90	0.84
Temporo-parieto-occipital channels	Delta theta	0.1–0.7 s	0.87	0.16	0.91/0.84	0.94	0.86	0.88	0.89
		0.1–0.5 s	0.83	0.20	0.84/0.80	0.92	0.84	0.86	0.86
		0.1–0.3 s	0.86	0.17	0.88/0.81	0.92	0.87	0.89	0.89
	Delta	0.1–0.7 s	0.88	0.19	0.89/0.89	0.89	0.89	0.92	0.89
		0.1–0.5 s	0.84	0.21	0.87/0.89	0.89	0.83	0.87	0.82
		0.1–0.3 s	0.83	0.19	0.84/0.78	0.92	0.84	0.87	0.86
	Theta	0.1–0.4 s	0.66	0.25	0.72/0.67	0.79	0.65	0.65	0.69
	Low theta	0.1–0.4 s	0.69	0.22	0.75/0.61	0.85	0.69	0.71	0.75

ROI: region of interest, Acc: accuracy, Acc_std: accuracy standard deviation, TP/TN: true positive/true negative.

Table 3. Classification metrics for auditory target stimulation after running spatial-spectral-temporal searchlight analyses.

	Auditory target								
ROI	Frequency band	Time windows	Acc	Acc_std	TP/TN	AUC	f1 score	Precision	Recall
All channels	Delta theta	0.1–0.7 s	0.80	0.23	0.74/0.91	0.82	0.76	0.84	0.72
		0.1–0.5 s	0.77	0.22	0.76/0.74	0.86	0.77	0.76	0.84
		0.1–0.3 s	0.71	0.21	0.64/0.72	0.82	0.66	0.71	0.68
	Delta	0.1–0.7 s	0.76	0.23	0.74/0.82	0.84	0.69	0.74	0.69
		0.1–0.5 s	0.74	0.22	0.69/0.80	0.79	0.69	0.75	0.69
		0.1–0.3 s	0.69	0.25	0.66/0.75	0.76	0.63	0.70	0.62
	Theta	0.1–0.4 s	0.72	0.21	0.68/0.76	0.85	0.70	0.79	0.68
	Low theta	0.1–0.4 s	0.73	0.19	0.66/0.74	0.85	0.69	0.74	0.71
Fronto-central channels	Delta theta	0.1–0.7 s	0.85	0.17	0.82/0.87	0.88	0.81	0.85	0.82
		0.1–0.5 s	0.76	0.24	0.75/0.84	0.88	0.70	0.75	0.71
		0.1–0.3 s	0.68	0.28	0.76/0.62	0.81	0.70	0.69	0.77
	Delta	0.1–0.7 s	0.77	0.22	0.74/0.77	0.81	0.72	0.78	0.72
		0.1–0.5 s	0.75	0.23	0.71/0.78	0.81	0.72	0.76	0.72
		0.1–0.3 s	0.64	0.26	0.62/0.66	0.69	0.57	0.59	0.61
	Theta	0.1–0.4 s	0.74	0.24	0.69/0.75	0.81	0.72	0.75	0.72
	Low theta	0.1–0.4 s	0.63	0.25	0.59/0.70	0.74	0.58	0.61	0.61
Temporo-parieto-occipital channels	Delta theta	0.1–0.7 s	0.79	0.20	0.75/0.84	0.87	0.78	0.85	0.77
		0.1–0.5 s	0.84	0.19	0.88/0.77	0.92	0.84	0.82	0.89
		0.1–0.3 s	0.75	0.23	0.78/0.68	0.87	0.72	0.73	0.76
	Delta	0.1–0.7 s	0.72	0.23	0.68/0.77	0.78	0.69	0.73	0.71
		0.1–0.5 s	0.75	0.19	0.65/0.83	0.79	0.67	0.75	0.65
		0.1–0.3 s	0.65	0.25	0.65/0.70	0.65	0.62	0.66	0.63
	Theta	0.1–0.4 s	0.77	0.22	0.76/0.75	0.86	0.75	0.77	0.78
	Low theta	0.1–0.4 s	0.84	0.18	0.79/0.84	0.95	0.82	0.88	0.81

ROI: region of interest, Acc: accuracy, Acc_std: accuracy standard deviation, TP/TN: true positive/true negative.

prediction accuracy rate than low theta, especially for event-related visual target ITPC.

To understand which channels contribute most to classification performances, accuracy metrics were obtained for each channel and plotted as a topography (figure 5). The topographies were plotted for each frequency band and time window where the best accuracy has been achieved for both paradigms and highlight the distinguishing features of visual and auditory event-related ITPC to detect PDD. As

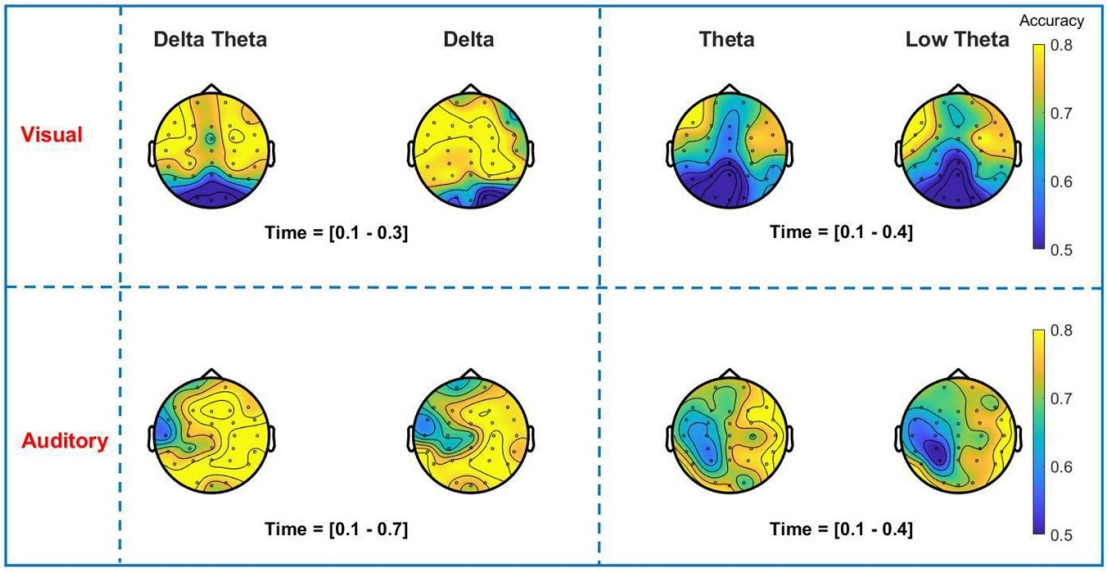

Figure 5. Topographic distributions of accuracy values for all frequency ranges and time windows where the highest value has been achieved upon application of both visual and auditory target stimulations separately.

seen from the figure, mostly fronto-central channels have contributed to the classification performance for all frequency bands upon application of visual target stimulation. On the other hand, there are somewhat widespread accuracy values over the TPO region, especially for theta and low theta upon application of auditory target stimulation whereas in delta and delta-theta combined almost all locations have contributed.

In the case fronto-central ROI was used as features, event-related visual delta and delta-theta combined have slightly similar accuracy values to the other ROIs, however, the accuracies for event-related visual theta and low theta have much higher than the other ROIs. On the other hand, when TPO channels were used as features, there is an appreciable increase in the accuracy of low theta for event-related auditory ITPC. Among all results of searchlight analyses performed for different ROIs, frequency, and time of interest, the best accuracy which is supporting our hypothesis has been obtained for the delta (1–4 Hz) frequency band and at 0.1–0.3 s time window over the fronto-central region upon application of visual target stimulation to classify HC and PDD.

Figure 6 depicts the results of the classification by means of confusion matrix, recall, precision, and accuracy metrics. The confusion matrix shows that the classifier is slightly better at predicting HC (0.95) than it is at predicting PDD (0.94) with 0.95 recall, 0.96 precision, and 0.94 accuracy.

4. Discussion

To our knowledge, this is the first study that attempts to classify PDD by means of EROs during cognitive tasks and compare the classification performances of two different modalities. The current study evaluated the ITPC upon target stimulation of visual and auditory oddball paradigms with varying analyses of searchlight to understand which features have more contribution to identifying PDD. For this purpose, LDA was used as a classifier.

The results revealed that we were able to classify PDD successfully. The remarkable performances were exhibited in different frequency bands and at different time windows. The most important observations of spatial-spectral-temporal searchlight analyses can be summarized as follows;

(1) The results from the classification analyses of the event-related visual target ITPC in the delta frequency band and at 0.1–0.3 s time window demonstrate the highest accuracy (0.94) for identifying PDD in the case that fronto-central channels were used as features.
(2) Visual target ITPC features contribute more to the differentiation of PDD compared to Auditory target ITPC in delta and delta-theta combined frequency bands.
(3) Low theta frequency band performs better in visual target stimulation over fronto-central channels. However, if auditory target stimulation is used, then TPO channels are more helpful to detect PDD, but still have lower performance than the case where visual target stimulation was used.

These results were not surprising since various studies reported abnormalities in delta and theta EROs of visual and auditory modality in all stages of the PDD continuum including cognitively normal PD (Emek Savaş *et al* 2017, Güntekin *et al* 2018,

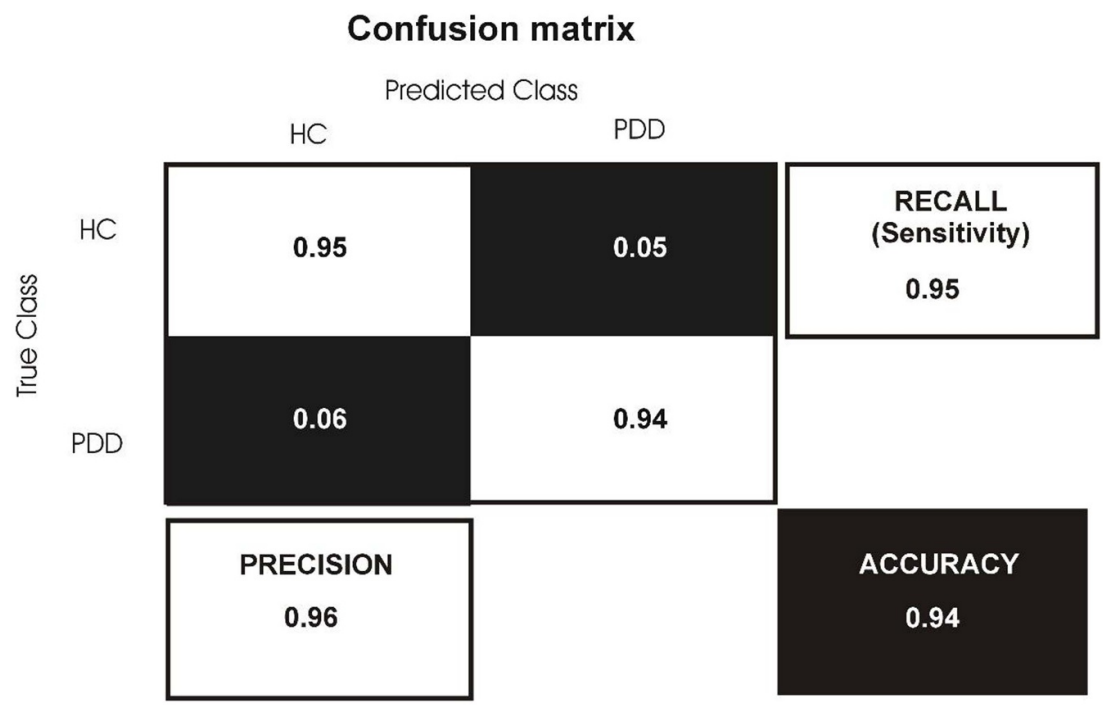

Figure 6. The classification metrics that were obtained for the delta (1–4 Hz) frequency band and at 0.1–0.3 s time window (HC vs PDD).

Solís-Vivanco *et al* 2018), PD with MCI (Güntekin *et al* 2018, Yener *et al* 2019) and PDD (Güntekin *et al* 2018, 2020) as well as cognitive impairments due to non-Parkinsonian pathologies (MCI, AD) (Yener *et al* 2007, 2008, 2009, 2012, 2013, 2016, Kurt *et al* 2014, Tulay *et al* 2020). Moreover, there are a few studies that have revealed that PD and HC can be classified by delta and theta brain responses to different cognitive tasks. Singh *et al* (2018) evaluated mid-frontal theta activity during the Simon reaction-time task and reported that post-error mid-frontal theta could be used to classify HC vs. PD with a near-chance sensitivity but reasonable specificity. Also, Cavanagh *et al* (2018) showed that brain responses to novel sounds differentiate PD from HC with a maximum accuracy of 82%, primarily in the delta band. PD has also been distinguished from Dementia with Lewy bodies by means of visual delta and theta powers via ROC curve analysis (Rosenblum *et al* 2022).

Among the aforementioned previous ERO studies, Güntekin *et al* (2020) mainly focused on the theta band, whereas in the current study, we evaluated both delta and theta during the visual and auditory stimulus. Moreover, Güntekin *et al* (2018) investigated the role of delta oscillatory response during a single modality (i.e. auditory oddball) and they used different EEG features instead of phase information of EEG, which was affected in dementia. However, in the present study, visual and auditory modalities for delta and theta frequency were evaluated to detect the best spatial-spectral-temporal feature set among different cognitive task modalities, frequency bands, time ranges, and brain areas to classify PDD. In line with these pioneering studies, our results also demonstrated quite substantial classification results for delta-theta frequency bands during the cognitive task. Furthermore, we showed that the results of the classification might vary according to parameters that were used in the analysis, such as exact frequency band limits, chosen time window, modality of the used task, and, accordingly locality of the recorded EEG signal. In this respect, the most substantial classification outcomes of the current study will be discussed in the following paragraphs by comparing the results of mentioned different parameters.

4.1. Phase-locking of event-related responses in delta frequency during visual target stimuli differentiates PDD from HC

In the current study, spatial-spectral-temporal searchlight analyses revealed that visual modality contributes to the classification of PDD more than auditory modality in general (please see tables 2 and 3) and these findings are fully in line with the previous researches that reported visual impairment on cognitive processes in PD (Arrigo *et al* 2017). Correspondingly, frontal lobe dysfunction occurs in the early stages of PD (de la Fuente-fernández 2012, Biundo *et al* 2016). Therefore, finding the highest classification performances for delta and theta phase-locking factor over the fronto-central region during visual modality is an expected result for PDD with progressive visual system impairment. Additionally, according to Güntekin *et al* (2022), in line with our

finding, slow frequency responses (<8 Hz) during visual oddball task were more sensitive in detecting cognitive impairment (as a physiological biomarker) than other tasks (and frequencies). Although Güntekin *et al* (2022) concluded this for Alzheimer's dementia, it is quite consistent with our findings in terms of showing that slow oscillatory responses during the visual oddball task are important in the classification of dementia.

Although the best classification performance to detect PDD was achieved with ITPC of event-related responses in the delta frequency band and at 0.1–0.3 time window during visual target stimuli over fronto-central channels (0.94), in the case where all channels contributed to the classification process, almost the same accuracy value has obtained for the equal frequency-time points (0.93). Moreover, when the slow oscillatory response (1–7 Hz) to visual modality over fronto-central locations was used as features, the classifier performances exceeded 0.90 s in both 0.1–0.5 and 0.1–0.3 time windows and reached 0.91 and 0.92, respectively. The predominance of the fronto-central region in visual stimuli also seems to be in accordance with previous studies (Emek Savaş *et al* 2017, Yener *et al* 2019).

On the other hand, in the auditory modality, the performance of the classifier is lower than the visual modality for the same spatial-spectral-temporal interests. However, for auditory modality, when the slow oscillatory response in a wider time range (0.1–0.7 s) was used as a feature, the accuracy values reached the same level as visual modality over all locations (0.80), and fronto-central locations (0.85). Cavanagh *et al* (2018) also reported similar accuracy (82%) in delta responses to detect PD for auditory stimuli as well. Furthermore, in line with current findings, Güntekin *et al* (2018) showed a gradual decrease of delta responses at 0–0.6 s time window and at overall locations in the dementia spectrum of PD during the auditory oddball task. Güntekin *et al* (2020) also revealed that PD-MCI and PDD had lower theta phase-locking and power compared to HC at overall locations. In contrast, the differentiation between HC and cognitively normal PD was more specific to frontal-central areas. Therefore, our results may indicate that a wider time window in the slower oscillations may provide a higher level of accuracy for the auditory modality in the classification of PDD.

4.2. Low theta has a discriminative role in different regions upon application of visual and auditory target

According to the literature, theta oscillatory responses are associated with several cognitive functions (Başar-Eroglu *et al* 1992, Demiralp *et al* 1994, Yener *et al* 2007). These studies showed that theta responses increase with the increase of cognitive functions. Therefore, it is highly expected to find the contribution of theta phase-locking to predict PDD in the current study.

Although misclassification is most prominent for theta and low theta responses of both visual and auditory stimulation, promising accuracy values has obtained for low theta responses rather than theta responses. However, recent studies reported that the wider range of theta (from 4 Hz to 7–8 Hz) helps to discriminate PD over the frontal-central area (Singh *et al* 2018, Güntekin *et al* 2020) and PDD over all locations (Güntekin *et al* 2020). On the other hand, the current study revealed a relatively low level of accuracy for the same frequency and ROI during visual (0.69) and auditory (0.72) target stimuli.

Interestingly, the results of the current study revealed that ITPC of event-related responses in the low theta frequency band during visual target stimuli over fronto-central channels showed a slightly greater accuracy level (0.87) than the full range theta frequency band showed (0.82). On the other hand, in auditory modality classification, performance for the low theta frequency band reached the same levels as visual modality over the TPO region (0.84), where the classifier is better at predicting PDD (0.84) than it is at predicting HC (0.79). This modality-specific classification success at differentiated locations could provide us with the initial information to be used in facilitating the EEG recording process in the clinical setting, such as recording EEG only from certain locations depending on task modality.

5. Conclusion

The current study is the pioneering study in the classification of PDD by means of EROs during visual and auditory stimuli and has shown the valuable contributions of delta and theta phase-locking factors to detect the disease. The classification performance results of the current study revealed that if the visual stimuli are applied to PDD, the delta and theta phase-locking factor over the fronto-central region has a substantial contribution to detecting the disease whereas if auditory stimuli are applied, the phase-locking factor in low theta over the TPO region and in a wider range of frequency (1–7 Hz) over the fronto-central region classify HC and PDD with better performances.

Although the results have revealed a promising classification rate, several biases/challenges/limitations can be mentioned. As a major problem, it is not possible to understand whether the current findings, which confirm the results of previous studies about the decrement of slow oscillatory responses in different phases of PD and AD are disease-specific (Güntekin *et al* 2022). More explicitly, at this stage, it is not possible to conclude yet whether our results reflect the different phases of cognitive decline in PD patients (i.e. subtyping) or are even disease-specific (i.e. AD vs PD). To overcome this limitation,

it absolutely would be better to include different groups of PD patients with different cognitive statuses and also other types of dementia, such as AD, in future studies. In such a future study design, as a next step, it would be possible to test how sensitive the spatial-spectral-temporal specific classification finding found here is for other subtypes of PD and other types of dementia. Additionally, this inclusion also will be helpful for early diagnosis of the diseases.

Moreover, the fact that patients are using drugs will undoubtedly affect the classification performance to predict PDD since medication affects the auditory perception of PD (Georgiev *et al* 2015). We should also acknowledge that the current study addressed the PDD classification with a small sample set and imbalanced gender categories.

Data availability statement

The data cannot be made publicly available upon publication because the cost of preparing, depositing and hosting the data would be prohibitive within the terms of this research project. The data that support the findings of this study are available upon reasonable request from the authors.

Conflict of interest

The authors declare that there is no conflict of interests regarding the publication of this paper.

ORCID iDs

Emine Elif Tülay https://orcid.org/0000-0003-0150-5476
Ebru Yıldırım https://orcid.org/0000-0002-7715-3035
Tuba Aktürk https://orcid.org/0000-0002-7555-3801
Bahar Güntekin https://orcid.org/0000-0002-0860-0524

References

Aarsland D, Creese B, Politis M, Chaudhuri K R, Ffytche D H, Weintraub D and Ballard C 2017 Cognitive decline in Parkinson disease *Nat. Rev. Neurol.* **13** 217–31
Aljalal M, Aldosari S A, AlSharabi K, Abdurraqeeb A M and Alturki F A 2022 Parkinson's disease detection from resting-state EEG signals using common spatial pattern, entropy, and machine learning techniques *Diagnostics* **12** 1033
Alzubaidi M S, Shah U, Dhia Zubaydi H, Dolaat K, Abd-Alrazaq A A, Ahmed A and Househ M 2021 The role of neural network for the detection of Parkinson's disease: a scoping review *Healthcare* **9** 740
Anjum M F, Dasgupta S, Mudumbai R, Singh A, Cavanagh J F and Narayanan N S 2020 Linear predictive coding distinguishes spectral EEG features of Parkinson's disease *Parkinsonism Relat. Disord.* **79** 79–85
Arrigo A *et al* 2017 Visual system involvement in patients with newly diagnosed Parkinson disease *Radiology* **285** 885–95
Başar E, Başar-Eroglu C, Karakaş S and Schürmann M 2001 Gamma, alpha, delta, and theta oscillations govern cognitive processes *Int. J. Psychophysiol.* **39** 241–8 (PMID: 11163901)
Başar E, Demiralp T, Schürmann M, Başar-Eroğlu C and Ademoğlu A 1999 Oscillatory brain dynamics, wavelet analysis, and cognition *Brain Lang.* **66** 146–83
Başar-Eroglu C, Başar E, Demiralp T and Schürmann M 1992 P300-response: possible psychophysiological correlates in delta and theta frequency channels *A Review. Int. J. Psychophysiol.* **13** 161–79 (PMID: 1399755)
Başar-Eroğlu C and Demiralp T 2001 Event-related theta oscillations: an integrative and comparative approach in the human and animal brain *Int. J. Psychophysiol.* **39** 167–95
Bestwick J P, Auger S D, Schrag A E, Grosset D G, Kanavou S, Giovannoni G, Lees A J, Cuzick J and Noyce A J 2021 Optimising classification of Parkinson's disease based on motor, olfactory, neuropsychiatric and sleep features *npj Parkinson's Dis.* **7** 87
Bind S, Tiwari A K and Sahani A K 2015 A survey of machine learning based approaches for Parkinson disease prediction *Int. J. Comput. Sci. Inf. Technol.* **6** 1648–55 (Corpus ID: 1896816)
Biundo R, Weis L and Antonini A 2016 Cognitive decline in Parkinson's disease: the complex picture *npj Parkinson's Dis.* **2** 16018
Cavanagh J F, Kumar P, Mueller A A, Richardson S P and Mueen A 2018 Diminished EEG habituation to novel events effectively classifies Parkinson's patients *Clin. Neurophysiol.* **129** 409–18
Chang K-H *et al* 2022 Evaluating the different stages of Parkinson's disease using electroencephalography with Holo-Hilbert spectral analysis *Front. Aging Neurosci.* **14** 832637
Chaturvedi M, Hatz F, Gschwandtner U, Bogaarts J G, Meyer A, Fuhr P and Roth V 2017 Quantitative EEG (QEEG) measures differentiate Parkinson's disease (PD) patients from healthy controls (HC) *Front. Aging Neurosci.* **9** 3 (PMID: 28167911; PMCID: PMC5253389)
Chen Z S, Kulkarni P, Galatzer-Levy I R, Bigio B, Nasca C and Zhang Y 2022 Modern views of machine learning for precision psychiatry (arXiv:2204.01607)
Coelho B F O, Massaranduba A B R, Souza C A, dos S, Viana G G, Brys I and Ramos R P 2023 Parkinson's disease effective biomarkers based on Hjorth features improved by machine learning *Expert Syst. Appl.* **212** 118772
Daniel S E and Lees A J 1993 Parkinson's Disease Society Brain Bank, London: overview and research *J. Neural Transm. Suppl.* **39** 165–72 (PMID: 8360656)
de la Fuente-fernández R 2012 Frontostriatal cognitive staging in Parkinson's disease *Parkinson's Dis.* **2012** 561046 (PMID: 22191070; PMCID: PMC3236592)
Delorme A and Makeig S 2004 EEGLAB: an open source toolbox for analysis of single-trial EEG dynamics including independent component analysis *J. Neurosci. Methods.* **134** 9–21
Demiralp T, Ademoglu A, Comerchero M and Polich J 2001 Wavelet analysis of P3a and P3b *Brain Topogr.* **13** 251–67
Demiralp T, Ademoglu A, Istefanopulos Y, Başar-Eroğlu C and Başar E 2000 Wavelet analysis of oddball P300 *Int. J. Psychophysiol.* **39** 221–7
Demiralp T, Başar-Eroglu C, Rahn E and Başar E 1994 Event-related theta rhythms in cat hippocampus and prefrontal cortex during an omitted stimulus paradigm *Int. J. Psychophysiol.* **18** 35–48
Emek Savaş D D, Özmüş G, Güntekin B, Dönmez Çolakoğlu B, Çakmur R, Başar E and Yener G G 2017 Decrease of delta oscillatory responses in cognitively normal Parkinson's disease *Clin. EEG Neurosci.* **48** 355–64
Emre M *et al* 2007 Clinical diagnostic criteria for dementia associated with Parkinson's disease *Mov. Disorders* **22** 1689–707 (PMID: 17542011)
Folstein M F, Folstein S E and McHugh P R 1975 Mini-mental state *J. Psychiatr. Res.* **12** 189–98

Georgiev D, Jahanshahi M, Dreo J, Cuš A, Pirtošek Z and Repovš G 2015 Dopaminergic medication alters auditory distractor processing in Parkinson's disease *Acta Psychol.* **156** 45–56

Güngen C, Ertan T, Eker E, Yaşar R and Engin F 2002 Standardize Mini Mental test'in türk toplumunda hafif demans tanisinda geçerlik ve güvenilirliği [Reliability and validity of the standardized Mini Mental State Examination in the diagnosis of mild dementia in Turkish population] *Turk Psikiyatri Derg.* **13** 273–81 (PMID: 12794644)

Güntekin B *et al* 2018 Cognitive impairment in Parkinson's disease is reflected with gradual decrease of EEG delta responses during auditory discrimination *Front. Psychol.* **9** 170

Güntekin B *et al* 2022 Are there consistent abnormalities in event-related EEG oscillations in patients with Alzheimer's disease compared to other diseases belonging to dementia? *Psychophysiology* **59** e13934 (PMID: 34460957)

Güntekin B, Aktürk T, Yıldırım E, Yılmaz N H, Hanoğlu L and Yener G 2020 Abnormalities in auditory and visual cognitive processes are differentiated with theta responses in patients with Parkinson's disease with and without dementia *Int. J. Psychophysiol.* **153** 65–79

Güntekin B and Başar E 2016 Review of evoked and event-related delta responses in the human brain *Int. J. Psychophysiol.* **103** 43–52 (PMID: 25660301)

Harmony T 2013 The functional significance of delta oscillations in cognitive processing *Front. Integr. Neurosci.* **7** 83

Hassin-Baer S, Cohen O S, Israeli-Korn S, Yahalom G, Benizri S, Sand D, Issachar G, Geva A B, Shani-Hershkovich R and Peremen Z 2022 Identification of an early-stage Parkinson's disease neuromarker using event-related potentials, brain network analytics and machine-learning *PLoS One* **17** e0261947

Hely M A, Reid W G J, Adena M A, Halliday G M and Morris J G L 2008 Sydney multicenter study of Parkinson's disease: the inevitability of dementia at 20 years *Mov. Disorders* **23** 837–44

Herrmann C S, Grigutsch M and Busch N A 2005 EEG oscillations and wavelet analysis *Event-related Potentials: A Methods Handbook* ed T C Handy (Cambridge, MA: MIT Press) pp 229–59 Corpus ID: 117188639

Hinnell C and Chaudhuri K R 2009 The effect of non-motor symptoms on quality of life in Parkinson's disease *Eur. Neurol. Rev.* **4** 29–33

Hoehn M M and Yahr M D 1967 Parkinsonism: onset, progression, and mortality *Neurology* **57** S11–26

Karakaş S 2020 A review of theta oscillation and its functional correlates *Int. J. Psychophysiol.* **157** 82–99 (PMID: 32428524)

Khachnaoui H, Mabrouk R and Khlifa N 2020 Machine learning and deep learning for clinical data and PET/SPECT imaging in Parkinson's disease: a review *IET Image Process.* **14** 4013–26

Khoshnevis S A and Sankar R 2021 Classification of the stages of Parkinson's disease using novel higher-order statistical features of EEG signals *Neural Comput. Appl.* **33** 7615–27

Klimesch W 1999 EEG alpha and theta oscillations reflect cognitive and memory performance: a review and analysis *Brain Res. Rev.* **29** 169–95

Kurt P, Emek-Savas D D, Batum K, Turp B, Güntekin B, Karsidag S and Yener G G 2014 Patients with mild cognitive impairment display reduced auditory event related delta oscillatory responses *Behav. Neurol.* **2014** 268967

Maitín A M, García-Tejedor A J and Muñoz J P R 2020 Machine learning approaches for detecting Parkinson's disease from EEG analysis: a systematic review *Appl. Sci.* **10** 8662

Makeig S, Debener S, Onton J and Delorme A 2004 Mining event-related brain dynamics *Trends Cogn. Sci.* **8** 204–10

Mei J, Desrosiers C and Frasnelli J 2021 Machine learning for the diagnosis of Parkinson's disease: a review of literature *Front. Aging Neurosci.* **13** 633752

Morris J C 1993 The clinical dementia rating (CDR): current version and scoring rules *Neurology* **43** 2412–4

Morris J C 1997 Clinical dementia rating: a reliable and valid diagnostic and staging measure for dementia of the Alzheimer type *Int. Psychogeriatr.* **9** 173–8

Movement Disorder Society Task Force on Rating Scales for Parkinson's Disease 2003 The unified Parkinson's disease rating scale (UPDRS): status and recommendations *Mov. Disorders* **18** 738–50

Oh S L, Hagiwara Y, Raghavendra U, Rajamanickam Yuvaraj N, Arunkumar M, Murugappan U and Acharya R 2020 A deep learning approach for Parkinson's disease diagnosis from EEG signals *Neural Comput. Appl.* **32** 10927–33

Oostenveld R, Fries P, Maris E and Schoffelen J-M 2011 FieldTrip: open source soft-ware for advanced analysis of MEG, EEG, and invasive electrophysiological data *Comput. Intell. Neurosci.* **2011** 156869

Parker D M and Crawford J R 2018 Assessment of frontal lobe dysfunction *A Handbook of Neuropsychological Assessment* ed J R Crawford, D M Parker and W W McKinlay (London: Routledge) pp 267–92

Pereira C R, Pereira D R, Weber S A T, Hook C, de Albuquerque V H C and Papa J P 2019 A survey on computer-assisted Parkinson's disease diagnosis *Artif. Intell. Med.* **95** 48–63 (PMID: 30201325)

Radha N, Sachin, Madhavan R M and Sameera Holy S 2021 Parkinson's disease detection using machine learning techniques *Rev. Argentina Clin. Psicol.* **30** 543–52

Raghavendra U, Acharya U R and Adeli H 2019 Artificial intelligence techniques for automated diagnosis of neurological disorders *Eur. Neurol.* **82** 41–64 (PMID: 31743905)

Rosenblum Y, Shiner T, Bregman N, Fahoum F, Giladi N, Maidan I and Mirelman A 2022 Event-related oscillations differentiate between cognitive, motor and visual impairments *J. Neurol.* **269** 3529–40

Saravanan S, Ramkumar K, Adalarasu K, Sivanandam V, Kumar S R, Stalin S and Amirtharajan R 2022 A systematic review of artificial intelligence (AI) based approaches for the diagnosis of Parkinson's disease *Arch. Comput. Methods Eng.* **29** 3639–53

Shirahige L, Berenguer-Rocha M, Mendonça S, Rocha S, Rodrigues M C and Monte-Silva K 2020 Quantitative electroencephalography characteristics for Parkinson's disease: a systematic review *J. Parkinson's Disease* **10** 455–70

Singh A, Richardson S P, Narayanan N and Cavanagh J F 2018 Mid-frontal theta activity is diminished during cognitive control in Parkinson's disease *Neuropsychologia* **117** 113–22

Solís-Vivanco R, Rodríguez-Violante M, Cervantes-Arriaga A, Justo-Guillén E and Ricardo-Garcell J 2018 Brain oscillations reveal impaired novelty detection from early stages of Parkinson's disease *NeuroImage Clin.* **18** 923–31

Stiasny-Kolster K, Mayer G, Schäfer S, Möller J C, Heinzel-Gutenbrunner M and Oertel W H 2007 The REM sleep behavior disorder screening questionnaire—a new diagnostic instrument *Mov. Disorders* **22** 2386–93

Tallon-Baudry C, Bertrand O, Delpuech C and Pernier J 1996 Stimulus specificity of phase-locked and non-phase-locked 40 Hz visual responses in human *J. Neurosci.* **16** 4240–9

Tanör Ö Ö 2011 Öktem sözel bellek süreçleri testi (Öktem-SBST) el kitabı Birinci Baskı (Ankara: Türk Psikolog Derneği Yayınları)

Tolosa E, Garrido A, Scholz S W and Poewe W 2021 Challenges in the diagnosis of Parkinson's disease *Lancet Neurol.* **20** 385–97

Treder M S 2020 MVPA-Light: a classification and regression toolbox for multi-dimensional data *Front. Neurosci.* **14** 289

Tremblay C, Mei J and Frasnelli J 2020 Olfactory bulb surroundings can help to distinguish Parkinson's disease from non-parkinsonian olfactory dysfunction *NeuroImage Clin.* **28** 102457

Tülay E E, Güntekin B, Yener G, Bayram A, Başar-Eroğlu C and Demiralp T 2020 Evoked and induced EEG oscillations to

visual targets reveal a differential pattern of change along the spectrum of cognitive decline in Alzheimer's disease *Int. J. Psychophysiol.* **155** 41–48

Tulay E E, Metin B, Tarhan N and Arıkan M K 2019 Multimodal neuroimaging: basic concepts and classification of neuropsychiatric diseases *Clin. EEG Neurosci.* **50** 20–33 PMID: 29925268

van Diepen R M and Mazaheri A 2018 The caveats of observing inter-trial phase-coherence in cognitive neuroscience *Sci. Rep.* **8** 2990

Vanegas M I, Ghilardi M F, Kelly S P and Blangero A 2018 Machine learning for EEG-based biomarkers in Parkinson's disease *IEEE Int. Conf. on Bioinformatics and Biomedicine (BIBM)* pp 2661–5

Wang Q, Meng L, Pang J, Zhu X and Ming D 2020 Characterization of EEG data revealing relationships with cognitive and motor symptoms in Parkinson's disease: a systematic review *Front. Aging Neurosci.* **12** 587396

Weingarten C P, Sundman M H, Hickey P and Chen N K 2015 Neuroimaging of Parkinson's disease: expanding views *Neurosci. Biobehav. Rev.* **59** 16–52

Williams-Gray C H, Mason S L, Evans J R, Foltynie T, Brayne C, Robbins T W and Barker R A 2013 The CamPaIGN study of Parkinson's disease: 10-year outlook in an incident population-based cohort *J. Neurol. Neurosurg. Psychiatry.* **84** 1258–64 (PMID: 23781007)

Yang C Y and Huang Y Z 2022 Parkinson's disease classification using machine learning approaches and resting-state EEG *J. Med. Biol. Eng.* **42** 263–70

Yang Y *et al* 2022 Artificial intelligence-enabled detection and assessment of Parkinson's disease using nocturnal breathing signals *Nat. Med.* **28** 2207–15

Yener G G, Emek-Savaş D D, Lizio R, Çavuşoğlu B, Carducci F, Ada E, Güntekin B, Babiloni C C and Başar E 2016 Frontal delta event-related oscillations relate to frontal volume in mild cognitive impairment and healthy controls *Int. J. Psychophysiol.* **103** 110–7

Yener G G, Fide E, Özbek Y, Emek-Savaş D D, Aktürk T, Çakmur R and Güntekin B 2019 The difference of mild cognitive impairment in Parkinson's disease from amnestic mild cognitive impairment: deeper power decrement and no phase-locking in visual event-related responses *Int. J. Psychophysiol.* **139** 48–58

Yener G G, Güntekin B, Öniz A and Başar E 2007 Increased frontal phase-locking of event-related theta oscillations in Alzheimer patients treated with cholinesterase inhibitors *Int. J. Psychophysiol.* **64** 46–52

Yener G G, Güntekin B, Orken D N, Tülay E, Forta H and Başar E 2012 Auditory delta event-related oscillatory responses are decreased in Alzheimer's disease *Behav. Neurol.* **25** 3–11

Yener G G, Kurt P, Emek-Savas D D, Güntekin B and Başar E 2013 Reduced visual event-related delta oscillatory responses in amnestic mild cognitive impairment *J. Alzheimer's Dis.* **37** 759–67

Yener G, Güntekin B and Başar E 2008 Event related delta oscillatory responses of Alzheimer patients *Eur. J. Neurol.* **15** 540–7

Yener G, Güntekin B, Tülay E and Başar E 2009 A comparative analysis of sensory visual evoked oscillations with visual cognitive event related oscillations in Alzheimer's disease *Neurosci. Lett.* **462** 193–7

Yesavage J A, Brink T L, Rose T L, Lum O, Huang V, Adey M and Leirer V O 1982 Development and validation of a geriatric depression screening scale: a preliminary report *J. Psychiatr. Res.* **17** 37–49

Yu Y-W, Tan C-H, Su H-C, Chien C-Y, Sung P-S, Lin T-Y, Lee T-L and Yu R-L 2022 A new instrument combines cognitive and social functioning items for detecting mild cognitive impairment and dementia in Parkinson's disease *Front. Aging Neurosci.* **14** 913958

Yuvaraj R, Rajendra Acharya U and Hagiwara Y 2018 A novel Parkinson's disease diagnosis index using higher-order spectra features in EEG signals *Neural Comput. Appl.* **30** 1225–35